Flood or Drought: How Do Aerosols Affect Precipitation?

Daniel Rosenfeld,[1]* Ulrike Lohmann,[2] Graciela B. Raga,[3] Colin D. O'Dowd,[4] Markku Kulmala,[5] Sandro Fuzzi,[6] Anni Reissell,[5] Meinrat O. Andreae[7]

Aerosols serve as cloud condensation nuclei (CCN) and thus have a substantial effect on cloud properties and the initiation of precipitation. Large concentrations of human-made aerosols have been reported to both decrease and increase rainfall as a result of their radiative and CCN activities. At one extreme, pristine tropical clouds with low CCN concentrations rain out too quickly to mature into long-lived clouds. On the other hand, heavily polluted clouds evaporate much of their water before precipitation can occur, if they can form at all given the reduced surface heating resulting from the aerosol haze layer. We propose a conceptual model that explains this apparent dichotomy.

Cloud physicists commonly classify the characteristics of aerosols and clouds into "maritime" and "continental" regimes, where "continental" has become synonymous with "aerosol-laden and polluted." Indeed, aerosol concentrations in polluted air masses are typically one to two orders of magnitude greater than in pristine oceanic air (Fig. 1) (*1*). However, before humankind started to change the environment, aerosol concentrations were not much greater (up to double) over land than over the oceans (*1*, *2*). Anthropogenic aerosols alter Earth's energy budget by scattering and absorbing the solar radiation that energizes the formation of clouds (*3*–*5*). Because all cloud droplets must form on preexisting aerosol particles that act as cloud condensation nuclei (CCN), increased aerosols also change the composition of clouds (i.e., the size distribution of cloud droplets). This, in turn, determines to a large extent the precipitation-forming processes.

Precipitation plays a key role in the climate system. About 37% of the energy input to the atmosphere occurs by release of latent heat from vapor that condenses into cloud drops and ice crystals (*6*). Reevaporation of clouds consumes back the released heat. When water is precipitated to the surface, this heat is left in the atmosphere and becomes available to energize convection and larger-scale atmospheric circulation systems.

The dominance of anthropogenic aerosols over much of the land area means that cloud composition, precipitation, the hydrological cycle, and the atmospheric circulation systems are all affected by both radiative and microphysical impacts of aerosols, and are likely to be in a different state relative to the pre-industrial era.

The Opposing Effects of Aerosols on Clouds and Precipitation

The radiative effects of aerosols on clouds mostly act to suppress precipitation, because they decrease the amount of solar radiation that reaches the land surface, and therefore cause less heat to be available for evaporating water and energizing convective rain clouds (*7*). The fraction of radiation that is not reflected back to space by the aerosols is absorbed into the atmosphere, mainly by carbonaceous aerosols, leading to heating of the air above the surface. This stabilizes the low atmosphere and suppresses the generation of convective clouds (*5*). The warmer and drier air thus produces circulation systems that redistribute the remaining precipitation (*8*, *9*). For example, elevated dry convection was observed to develop from the top of heavy smoke palls from burning oil wells (*10*). Warming of the lower troposphere by absorbing aerosols can also strengthen the Asian summer monsoon circulation and cause a local increase in precipitation, despite the global reduction of evaporation that compensates for greater radiative heating by aerosols (*11*). In the case of bright aerosols that mainly scatter the radiation back to space, the consequent surface cooling also can alter atmospheric circulation systems. It has been suggested that this mechanism has cooled the North Atlantic and hence pushed the Intertropical Convergence Zone southward, thereby contributing to the drying in the Sahel (*12*, *13*).

Aerosols also have important microphysical effects (*14*). Added CCN slow the conversion of cloud drops into raindrops by nucleating larger number concentrations of smaller drops, which are slower to coalesce into raindrops or rime onto ice hydrometeors (*15*, *16*). This effect was shown to shut off precipitation from very shallow and short-lived clouds, as in the case of

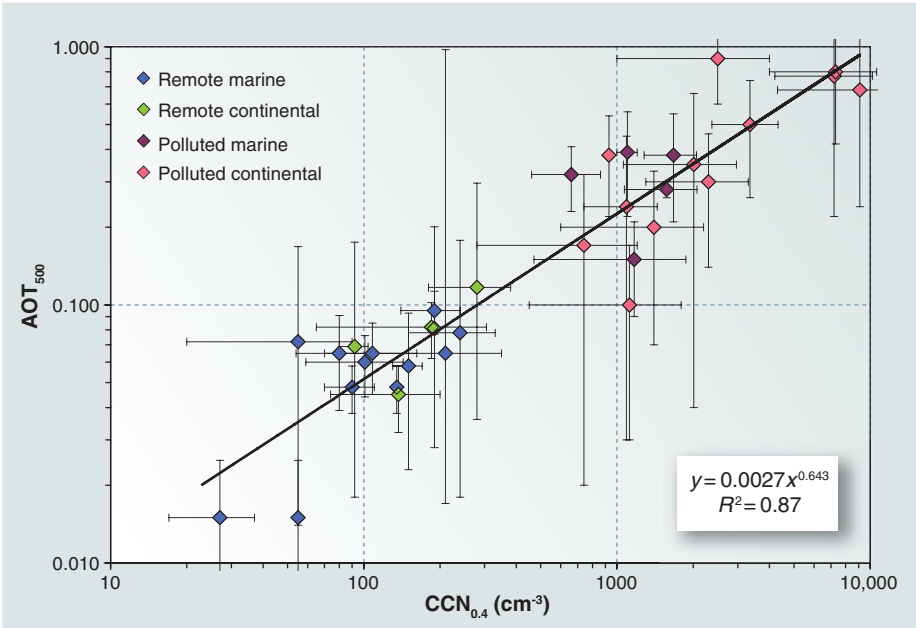

Fig. 1. Relations between observed aerosol optical thickness at 500 nm and CCN concentrations at supersaturation of 0.4% from studies where these variables have been measured simultaneously, or where data from nearby sites at comparable times were available. The error bars reflect the variability of measurements within each study (standard deviations or quartiles). The equation of the regression line between aerosol optical thickness (y) and $CCN_{0.4}$ (x) is given by the inset expression; R is the correlation coefficient. The aerosols exclude desert dust. [Adapted from (*1*)]

[1]Institute of Earth Sciences, Hebrew University of Jerusalem, Jerusalem 91904, Israel. [2]Institute for Atmospheric and Climate Science, ETH Zürich, 8092 Zürich, Switzerland. [3]Universidad Nacional Autónoma de México, Mexico City 04510, Mexico. [4]School of Physics and Centre for Climate and Air Pollution Studies, Environmental Change Institute, National University of Ireland, Galway, Ireland. [5]Department of Physics, University of Helsinki, Post Office Box 64, Helsinki 00014, Finland. [6]Istituto di Scienze dell'Atmosfera e del Clima–CNR, Bologna 40129, Italy. [7]Biogeochemistry Department, Max Planck Institute for Chemistry, Post Office Box 3060, D-55020 Mainz, Germany.

*To whom correspondence should be addressed. E-mail: daniel.rosenfeld@huji.ac.il

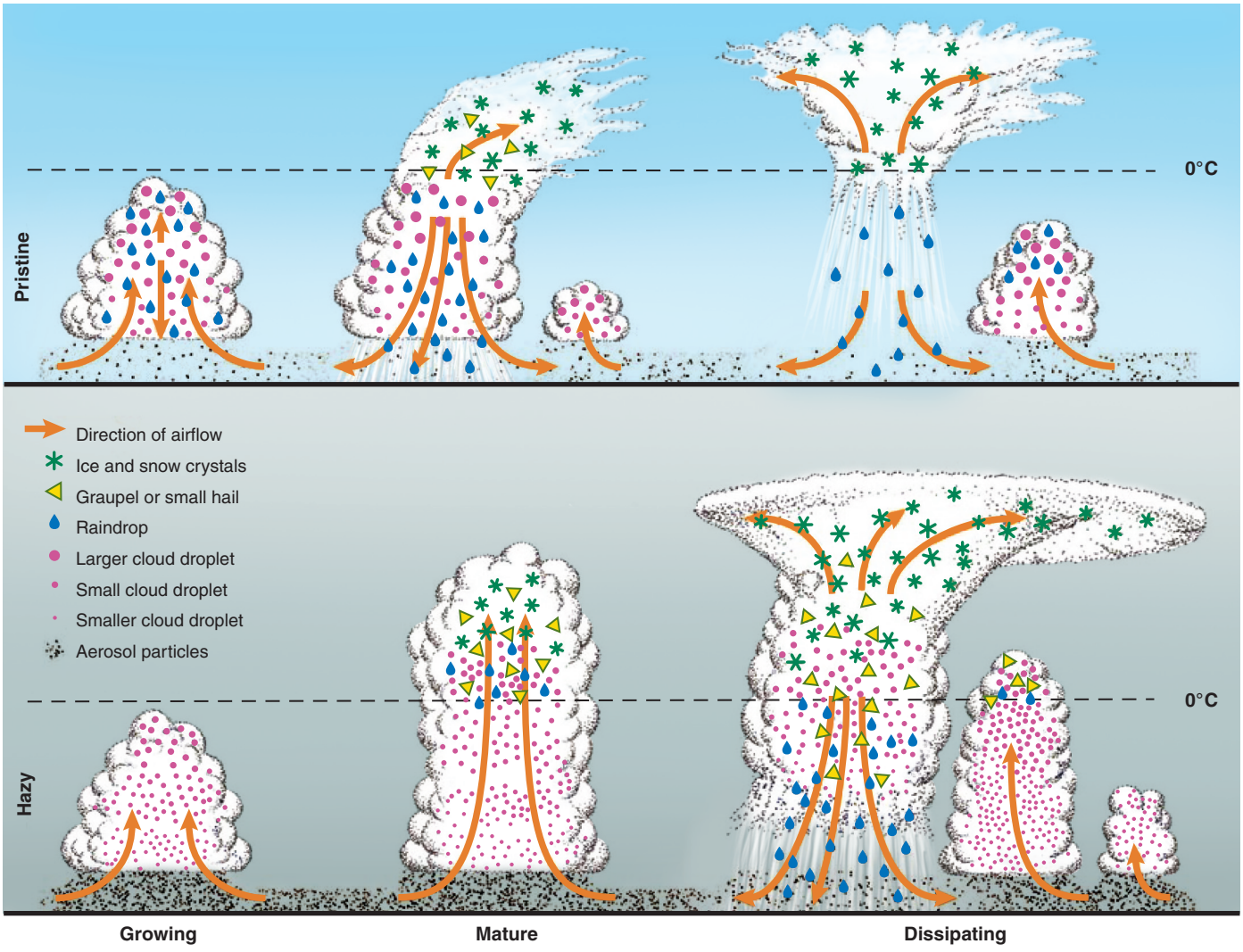

Fig. 2. Evolution of deep convective clouds developing in the pristine (top) and polluted (bottom) atmosphere. Cloud droplets coalesce into raindrops that rain out from the pristine clouds. The smaller drops in the polluted air do not precipitate before reaching the supercooled levels, where they freeze onto ice precipitation that falls and melts at lower levels. The additional release of latent heat of freezing aloft and reabsorbed heat at lower levels by the melting ice implies greater upward heat transport for the same amount of surface precipitation in the more polluted atmosphere. This means consumption of more instability for the same amount of rainfall. The inevitable result is invigoration of the convective clouds and additional rainfall, despite the slower conversion of cloud droplets to raindrops (*43*).

smoke from ship smokestacks in otherwise pristine clouds over the ocean (*17*). This created the expectation that polluted areas would suffer from reduced rainfall. On the other hand, it was expected that accelerating the conversion of cloud water to precipitation (i.e., increasing the autoconversion rate) by cloud seeding would enhance rainfall amounts. It turns out, however, that polluted areas are not generally drier, and rain enhancement by cloud seeding remains inconclusive (*18*, *19*).

With the advent of satellite measurements, it became possible to observe the larger picture of aerosol effects on clouds and precipitation. (We exclude the impacts of ice nuclei aerosols, which are much less understood than the effects of CCN aerosols.) Urban and industrial air pollution plumes were observed to completely suppress precipitation from 2.5-km-deep clouds over Australia (*20*). Heavy smoke from forest fires was observed to suppress rainfall from 5-km-deep tropical clouds (*21*, *22*). The clouds appeared to regain their precipitation capability when ingesting giant (>1 μm diameter) CCN salt particles from sea spray (*23*) and salt playas (*24*). These observations were the impetus for the World Meteorological Organization and the International Union of Geodesy and Geophysics to mandate an assessment of aerosol impact on precipitation (*19*). This report concluded that "it is difficult to establish clear causal relationships between aerosols and precipitation and to determine the sign of the precipitation change in a climatological sense. Based on many observations and model simulations the effects of aerosols on clouds are more clearly understood (particularly in ice-free clouds); the effects on precipitation are less clear."

A recent National Research Council report that reviewed "radiative forcing of climate change" (*25*) concluded that the concept of radiative forcing "needs to be extended to account for (1) the vertical structure of radiative forcing, (2) regional variability in radiative forcing, and (3) nonradiative forcing." It recommended "to move beyond simple climate models based entirely on global mean top of the atmosphere radiative forcing and incorporate new global and regional radiative and nonradiative forcing metrics as they become available." We propose such a new metric below.

How Can Slowing the Conversion of Cloud Droplets to Raindrops Enhance Rainfall?

A growing body of observations shows that submicrometer CCN aerosols decrease precipitation

from shallow clouds (*17*, *20*, *21*, *26*–*28*) and invigorate deep convective rain clouds with warm (> ~15°C) cloud base (*29*–*33*), although the impact on the overall rainfall amount is not easily detectable (*34*, *35*). These observations are supported by a large number of cloud-resolving model studies (*36*–*43*). The simulations also show that adding giant CCN to polluted clouds accelerates the autoconversion, mainly through nucleating large drops that rapidly grow into precipitation particles by collecting the other smaller cloud droplets (*44*). However, the autoconversion rate is not restored to that of pristine clouds (*42*).

Fundamentally, the amount of precipitation must balance the amount of evaporation at a global scale. Therefore, the consequence of aerosols suppressing precipitation from shallow clouds must be an increase in precipitation from deeper clouds. Such compensation can be accomplished not only at the global scale (*45*) but also at the cloud scale; that is, the clouds can grow to heights where aerosols no longer impede precipitation (*46*). All of this is consistent with the conceptual model shown in Fig. 2. This model suggests that slowing the rate of cloud droplet coalescence into raindrops (i.e., autoconversion) delays the precipitation of the cloud water, so that more water can ascend to altitudes where the temperature is colder than 0°C. Even if the total rainfall amount is not decreased by the increase in aerosols, delaying the formation of rain is sufficient to cause invigoration of cloud dynamics. By not raining early, the condensed water can form ice precipitation particles that release the latent heat of freezing aloft (*6*, *29*, *30*) and reabsorb heat at lower levels where they melt after falling.

The role of ice melting below the 0°C isotherm level in invigoration has been successfully modeled (*47*), although models also predict invigoration through increased aerosol loads even without ice processes (*43*). These model simulations suggest that the delay of early rain causes greater amounts of cloud water and rain intensities later in the life cycle of the cloud. The enhanced evaporative cooling of the added cloud water, mainly in the downdrafts, provides part of the invigoration by the mechanism of enhanced cold pools near the surface that push upward the ambient air. The greater cooling below and heating above lead to enhanced upward heat transport, both in absolute terms and normalized for the same amount of surface precipitation. The consumption of more convective available potential energy (CAPE) for the same rainfall amount would then be converted to an equally greater amount of released kinetic energy that could invigorate convection and lead to a greater convective overturning, more precipitation, and deeper depletion of the static instability (*6*). Simulations have shown that greater heating higher in the troposphere enhances the atmospheric circulation systems (*48*).

In clouds with bases near or above the 0°C isotherm, almost all the condensate freezes, even if it forms initially as supercooled raindrops in a low-CCN environment. Moreover, the slowing of the autoconversion rate by large concentrations of CCN can leave much of the cloud droplets airborne when strong updrafts thrust them above the homogeneous ice nucleation level of ~ –38°C, where they freeze into small ice particles that have no effective mechanism to coagulate and fall as precipitation. This phenomenon was observed by aircraft (*49*) and simulated for convective storms in west Texas (*50*) and the U.S. high plains (*51*). When the same simulation (*50*) was repeated with reduced CCN concentrations, the calculated rainfall amount increased substantially. The same model showed

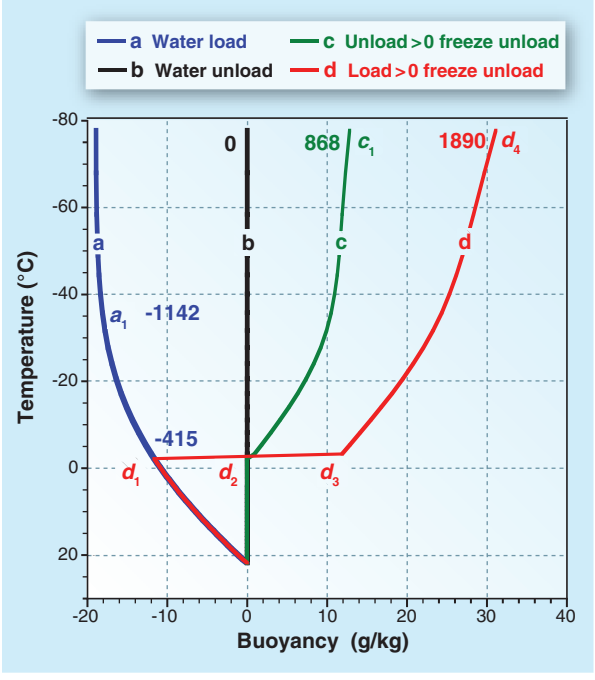

Fig. 3. The buoyancy of an unmixed adiabatically raising air parcel. The zero-buoyancy reference is the standard parcel: liquid water saturation, immediately precipitating all condensates without freezing (vertical line *b*). Cloud base is at 22°C and 960 hPa. The buoyancy of the following scenarios is shown: (*a*) suppressing rainfall and keeping all condensed water load, without freezing; (*b*) precipitating all condensed water, without freezing; (*c*) precipitating all condensates, with freezing at $T < -4$°C; (*d*) Suppressing precipitation until $T = -4$°C, and then freezing and precipitating all condensed water above that temperature. The released static energy (J kg^{-1}) with respect to reference line *b* is denoted by the numbers.

that adding small CCN aerosols in warm-base clouds has the opposite effect to that of cold-base clouds: increasing the precipitation amount by invigorating the convective overturning, while keeping the precipitation efficiency (i.e., surface precipitation divided by total cloud condensates) lower (*52*).

The invigoration due to aerosols slowing the autoconversion can be explained according to fundamental theoretical considerations of the pseudo-adiabatic parcel theory (Fig. 3). The CAPE measures the amount of moist static energy that is available to drive the convection. Its value is normally calculated with reference to a pseudo-adiabatic cloud parcel that rises while precipitating all its condensate in the form of rain, even at subfreezing temperatures.

Consider the case of a tropical air parcel that ascends from sea level with initial conditions of cloud base pressure of 960 hPa and temperature of 22°C. When not allowing precipitation, all the condensed water remains in the parcel and requires 415 J kg^{-1} to rise to the height of the –4°C isotherm (point d_1 in Fig. 3), which is the highest temperature at which freezing can practically occur in the atmosphere. Freezing all the cloud water would warm the air and add thermal buoyancy by an amount that would almost exactly balance the condensate load (d_2). When the ice hydrometeors precipitate from a parcel, it becomes more positively buoyant because of its reduced weight (d_3), so that the released convective energy at the top of the cloud (d_4) is the largest. Specifically, it is greater by ~1000 J kg^{-1} relative to the case where cloud water is precipitated as rain below the –4°C isotherm and as ice above that level (c_1). However, further delaying the conversion of cloud water into precipitation to greater heights above the 0°C level weakens the convection. In the extreme case of extending the suppression from the –4°C to the –36°C isotherm level (a_1), additional energy of 727 J kg^{-1} is invested in lifting the condensates. There is no effective mechanism for precipitating cloud water that glaciated homogeneously into small ice particles. This would prevent the unloading of the parcel, taking up even more convective energy and further suppressing the convection and the precipitation. In reality, cloud parcels always mix with the environment, but this applies equally to all the scenarios in Fig. 3, so that qualitatively the contrasting aerosol effects remain the same. Although the idealized calculations here are useful to establish the concepts, the exact calculations require running three-dimensional models on the full life cycle of convective cloud systems, followed by validation with detailed observations.

The importance of the aerosol control of the released convective energy by adding as much as 1000 J kg^{-1} can be appreciated by considering that CAPE averages ~1000 to 1500 J kg^{-1} in the Amazon (*30*). Simulations of aerosols invigorating peak updrafts by 20% (*37*, *52*) are

consistent with an increase of released convective energy by nearly 50%.

Role of Radiative Versus Microphysical Aerosol Effects

Until now, the radiative and microphysical impacts of aerosols on the climate system have been considered separately and independently; their various, often conflicting, influences have not been amenable to quantitative weighting on the same scale. Given the opposing microphysical and radiative effects on the vigor and rainfall amounts of deep warm-base convective clouds, there is a need to assess the combined effects of these two factors (*25*).

A quantitative comparison between the strengths of the radiative and microphysical effects of the aerosols is presented in Fig. 4. Because optically active aerosols are larger than 0.05 μm in radius, and because mature pollution aerosols of this or larger size can act as CCN (*53*), CCN concentrations generally increase with aerosol optical thickness (AOT) (Fig. 1). The empirical relationship between AOT and CCN is shown in Fig. 4 by AOT = 0.0027 × $(CCN_{0.4})^{0.64}$ (*1*), where $CCN_{0.4}$ is the concentration of CCN active at a supersaturation of 0.4%. The cloud droplet concentration N_c is proportional to $(CCN_{0.4})^k$, where k is typically smaller than 1. Using $k = 0.825$ relates 2000 cloud drops cm^{-3} to 10^4 $CCN_{0.4}$ cm^{-3}, which corresponds to AOT = 1. The value of k was inferred from Ramanathan *et al*. (*7*), although Freud *et al*. (*54*) imply that k is closer to 1. In turn, N_c was shown to be related to the depth above cloud base (D) required for onset of rain (*54*). This depth determines the thermodynamic track of the rising parcel (Fig. 3) and hence the vigor of the convection and the extent of convective overturning, which determines the rainfall amount produced by the cloud system throughout its life cycle. The cloudy parcel ascends along curve *a* in Fig. 3 as long as the cloud top has not reached D, and shifts to a track between curves *c* and *d* according to the amount of condensed water at that height.

The dependence of D on CCN is obtained by a compilation of aircraft measurements (*27*, *54*, *55*) that provides an approximate relation of $D = 80 + (4 \times CCN_{0.4})$. According to this relation, $CCN_{0.4}$ should reach ~1200 cm^{-3} for preventing rainout from typical tropical clouds before reaching the practical freezing temperature of –4°C, which is at $D \approx 5$ km. At this point the invigoration effect is at its maximum, where the cloud parcel follows curve *d* in Fig. 3. Adding CCN beyond this point suppresses the vigor of the convection by shifting the cloud parcel gradually from curve *d* to curve *a* in Fig. 3. This means that the microphysical effect on invigorating the convection has a maximum at moderate CCN concentrations. This maximum becomes smaller for cooler-base clouds, where the distance to the freezing level is shorter, so that fewer CCN are sufficient to suppress the onset of rain up to that level.

At the point of strongest microphysical invigoration, AOT is still at the modest value of ~0.25. Added aerosols increase the AOT and reduce the flux of solar energy to the surface, which energizes convection. As a result, with increasing aerosol loads beyond the optimum, the weakening of the microphysical invigoration is reinforced by the suppressive effect of reduced surface heating.

The interplay between the microphysical and radiative effects of the aerosols may explain the observations of Bell *et al*. (*33*), who showed that the weekly cycle of air pollution aerosols in the southeastern United States is associated with a weekday maximum and weekend minimum in the intensity of afternoon convective rainfall during summer. This was mirrored by a minimum in the midweek rainfall over the adjacent sea areas, reflecting an aerosol-induced modulation of the monsoonal convergence of air and its rising over land with return flow aloft to the ocean. This is a remarkable finding, as it suggests that the microphysical impacts of aerosols on invigorating warm-base deep clouds are not necessarily at the expense of other clouds in the same region, but can lead to changes in regional circulation that lead to greater moisture convergence and regional precipitation.

This weekly cycle emerged in the late 1980s and strengthened through the 1990s, along with the contemporary reversal of the dimming trend of solar radiation reaching the surface, which took place until the 1980s (*56*). This was likely caused by the reversal in the emissions trends of sulfates and black carbon (*57*). It is possible that the weekly cycle emerged when the overall aerosol levels decreased to the range where the microphysical impacts are dominant, as shown in Fig. 4.

Measuring Radiative and Microphysical Aerosol Effects with the Same Metric

The precipitation and the radiative effects of the aerosols (both direct and cloud-mediated) can be integrally measured when considering the combined changes in the energy of the atmosphere and the surface. The commonly used metrics are the radiative forcing at the top of the atmosphere (TOA) and at the BOA (bottom of the atmosphere, i.e., Earth's surface), measured in W m^{-2}. The atmospheric radiative forcing is the difference between TOA and BOA forcing (*7*). Here we propose a new metric, the aerosol thermodynamic forcing (TF) (*58*), representing the aerosol-induced change in the atmospheric energy budget that is not radiative in nature. In contrast to TOA radiative forcing, TF does not change the net Earth energy budget, but rather redistributes it internally; hence, TF can affect temperature gradients and atmospheric circulation. The main source of TF is the change in the amount of latent heat released by aerosol-induced changes in clouds and precipitation. It can be expressed as a change in latent heat flux (in units of W m^{-2}) in the atmospheric column.

The vertical distribution of the atmospheric heating is critically important because it determines the vertical lapse rate and hence the CAPE, which quantifies the ability to produce convective clouds and precipitation. Atmospheric radiative heating due to absorbing aerosols tends to reduce CAPE and thereby suppress the development of convective clouds, whereas the microphysical effects of aerosols allow a deeper exploitation of CAPE and hence invigoration of convection and associated precipitation.

All the components of the aerosol radiative (direct and cloud-

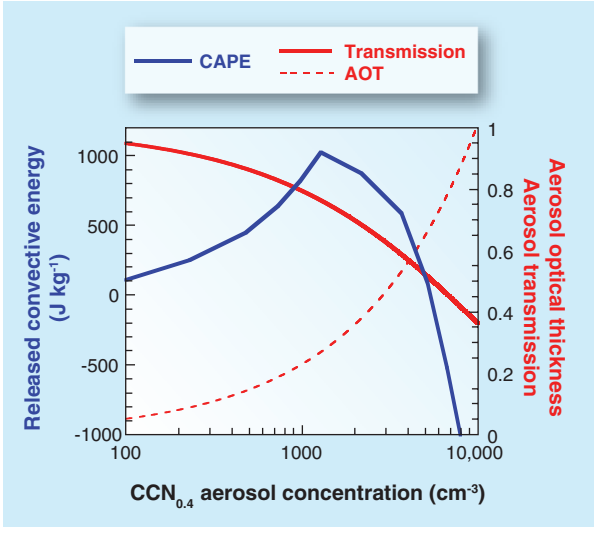

Fig. 4. Illustration of the relations between the aerosol microphysical and radiative effects. The aerosol optical thickness (AOT) is assumed to reach 1 at $CCN_{0.4} = 10^4$ cm^{-3} (dashed red line), which corresponds to nucleation of 2000 cloud drops cm^{-3}. The related transmission of radiation reaching the surface is shown by the solid red line. The vigor of the convection is shown by the blue line, which provides the released convective available potential energy (CAPE) of a cloud parcel that ascends to the cloud top near the tropopause. The calculation is based on the scheme in Fig. 3, with respect to curve *c* as the zero reference. Note that a maximum in CAPE occurs at $CCN_{0.4} \approx 1200$ cm^{-3}, which corresponds to the maximum cloud invigoration according to curve *d* of the scheme in Fig. 3. The AOT corresponding to the $CCN_{0.4}$ at the microphysical optimum is only 0.25. Adding aerosols beyond this point substantially decreases the vigor of the cloud because both microphysical and radiative effects work in the same direction: smaller release of convective energy aloft and less radiative heating at the surface.

mediated) and thermodynamic forcing and the resulting changes in CAPE can now be quantified as energy flux perturbations in units of W m^{-2}. Consider the example of smoke changing tropical convection from thermodynamic path *c* to path *d* in Fig. 3. At the end of the convective cycle, an additional 1000 J kg^{-1} are depleted from CAPE relative to convection under pristine conditions. The resultant increased convective overturning is likely to produce more rainfall and increase the temperature by converting more latent heat into sensible heat, at a rate of 29 W m^{-2} for each added millimeter of rainfall during 24 hours. This can be considered as a cloud-mediated TF of aerosols, which works to enhance rainfall and accelerate the hydrological cycle, resulting in a positive sign for TF. On the other hand, if the smoke becomes very thick, its radiative impact would be to reduce surface latent and sensible heating and warm the mid-troposphere. For example, an AOT of 1 induces a BOA forcing of –45 W m^{-2} in the Amazon (*5*). This stabilization of the atmosphere would cause less convection and depletion of CAPE, less rainfall, and a resulting deceleration of the hydrological cycle (*7*). Furthermore, too much aerosol can suppress the precipitation-forming processes to the extent of changing from thermodynamic path *d* to path *a* in Fig. 3 (see also Fig. 4), hence reversing the cloud-mediated TF of aerosols from positive to negative, adding to the negative radiative forcing.

Thermodynamic forcing can occur even without changing the surface rainfall: The energy change when polluted clouds develop along track *d* in Fig. 3, with respect to the pristine reference state shown in track *c*, would be defined as TF. In this case, the TF solely due to added release of latent heat of freezing is 2.44 W m^{-2} mm^{-1} day^{-1} of heating above the freezing level and the same amount of cooling due to melting below the melting level. This is a net vertical redistribution of latent heat. For an area-average rainfall of 20 mm day^{-1}, the TF scales to 48.8 W m^{-1}. In addition, we should consider the thermodynamic consequences of the aerosol-induced added rainfall due to increased convective overturning. This would convert latent heat to sensible heat at a rate of 29 W m^{-2} mm^{-1} day^{-1}. Such deeper consumption of CAPE would require a longer time for the atmosphere to recover for the next convective cycle, representing a temporal redistribution of heating and precipitation.

Concluding Thoughts

The next challenge will be to map the radiative and cloud-mediated thermodynamic forcing of the aerosols in the parameter space of AOT versus CCN. The good correlation between AOT and CCN means that, at least at large scales, the radiative and microphysical effects of aerosols on cloud physics are not free to vary independently (*1*), and hence mainly the diagonal of the parameter space is populated.

According to Fig. 4, there should be an optimum aerosol load in the tropical atmosphere that should lead to the most positive aerosol thermodynamic forcing, manifested as the most vigorous convection. This optimum probably occurs at AOT ≈ 0.25 and $CCN_{0.4}$ ≈ 1200 cm^{-3}. Remarkably, these fundamental considerations for AOT ≈ 0.25 for optimal cloud development were matched recently by observations in the Amazon (*59*).

This hypothesis reconciles the apparent contradictory reports that were reviewed in two major assessments (*18*, *19*) as impeding our overall understanding of cloud-aerosol impacts on precipitation and the climate system. The main cause for the previous uncertainties was the nonmonotonic character of competing effects, which is inevitable in a system that has an optimum. The new conceptual model outlined here improves our understanding and ability to simulate present and future climates. It also has implications for intentional weather and climate modification, which are being considered in the context of cloud seeding for precipitation enhancement and geoengineering. Testing this hypothesis is planned within the Aerosol Cloud Precipitation Climate (ACPC) initiative (*60*, *61*).

References and Notes

1. M. O. Andreae, *Atmos. Chem. Phys. Discuss.* **8**, 11293 (2008).
2. M. O. Andreae, *Science* **315**, 50 (2007).
3. U. Lohmann, J. Feichter, *Atmos. Chem. Phys.* **5**, 715 (2005).
4. V. Ramanathan *et al.*, *Proc. Natl. Acad. Sci. U.S.A.* **102**, 5326 (2005).
5. I. Koren, Y. J. Kaufman, L. A. Remer, J. V. Martins, *Science* **303**, 1342 (2004).
6. D. Rosenfeld, *Space Sci. Rev.* **125**, 149 (2006).
7. V. Ramanathan, P. J. Crutzen, J. T. Kiehl, D. Rosenfeld, *Science* **294**, 2119 (2001).
8. S. Menon, J. Hansen, L. Nazarenko, Y. F. Luo, *Science* **297**, 2250 (2002).
9. C. Wang, *J. Geophys. Res.* **109**, D03106 (2004).
10. Y. Rudich, A. Sagi, D. Rosenfeld, *J. Geophys. Res.* **108**, 10.1029/2003JD003472 (2003).
11. R. L. Miller, I. Tegen, J. Perlwitz, *J. Geophys. Res.* **109**, D04203 (2004).
12. L. D. Rotstayn, U. Lohmann, *J. Geophys. Res.* **107**, 10.1029/2002JD002128 (2002).
13. I. M. Held, T. L. Delworth, J. Lu, K. L. Findell, T. R. Knutson, *Proc. Natl. Acad. Sci. U.S.A.* **102**, 17891 (2005).
14. W. Cotton, R. Pielke, *Human Impacts on Weather and Climate* (Cambridge Univ. Press, Cambridge, 2007).
15. R. Gunn, B. B. Phillips, *J. Meteorol.* **14**, 272 (1957).
16. P. Squires, *Tellus* **10**, 256 (1958).
17. L. F. Radke, J. A. Coakley Jr., M. D. King, *Science* **246**, 1146 (1989).
18. National Research Council, *Critical Issues in Weather Modification Research* (National Academies Press, Washington, DC, 2003).
19. Z. Levin, W. Cotton, *Aerosol Pollution Impact on Precipitation: A Scientific Review. Report from the WMO/IUGG International Aerosol Precipitation Science Assessment Group (IAPSAG)* (World Meteorological Organization, Geneva, Switzerland, 2007).
20. D. Rosenfeld, *Science* **287**, 1793 (2000).
21. D. Rosenfeld, *Geophys. Res. Lett.* **26**, 3105 (1999).
22. D. Rosenfeld, W. L. Woodley, in *Cloud Systems, Hurricanes, and the Tropical Rainfall Measuring Mission (TRMM)*, W.-K. Tao, R. Adler, Eds. (American Meteorological Society, Boston, 2003), pp. 59–80.
23. D. Rosenfeld, R. Lahav, A. Khain, M. Pinsky, *Science* **297**, 1667 (2002); published online 15 August 2002 (10.1126/science.1073869).
24. Y. Rudich, O. Khersonsky, D. Rosenfeld, *Geophys. Res. Lett.* **29**, 10.1029/2002GL016055 (2002).
25. National Research Council, *Radiative Forcing of Climate Change: Expanding the Concept and Addressing Uncertainties* (National Academies Press, Washington, DC, 2005).
26. D. Rosenfeld, Y. J. Kaufman, I. Koren, *Atmos. Chem. Phys.* **6**, 2503 (2006).
27. D. Rosenfeld *et al.*, *J. Geophys. Res.* **113**, D15203 (2008).
28. M. O. Andreae *et al.*, *Science* **303**, 1337 (2004).
29. J. Molinié, C. A. Pontikis, *Geophys. Res. Lett.* **22**, 1085 (1995).
30. E. Williams *et al.*, *J. Geophys. Res.* **107**, 10.1029/2001JD000380 (2002).
31. I. Koren, Y. J. Kaufman, D. Rosenfeld, L. A. Remer, Y. Rudich, *Geophys. Res. Lett.* **32**, L14828 (2005).
32. J. C. Lin, T. Matsui, R. A. Pielke Sr., C. Kummerow, *J. Geophys. Res.* **111**, D19204 (2006).
33. T. L. Bell *et al.*, *J. Geophys. Res.* **113**, D02209 (2008).
34. D. M. Schultz, S. Mikkonen, A. Laaksonen, M. B. Richman, *Geophys. Res. Lett.* **34**, L22815 (2007).
35. T. Bell, D. Rosenfeld, *Geophys. Res. Lett.* **35**, L09803 (2008).
36. A. Khain, A. Pokrovsky, M. Pinsky, A. Seifert, V. Phillips, *J. Atmos. Sci.* **61**, 2963 (2004).
37. A. Khain, D. Rosenfeld, A. Pokrovsky, *Q. J. R. Meteorol. Soc.* **131**, 2639 (2005).
38. B. H. Lynn *et al.*, *Mon. Weather Rev.* **133**, 59 (2005).
39. C. Wang, *J. Geophys. Res.* **110**, D21211 (2005).
40. S. C. van den Heever, G. G. Carrió, W. R. Cotton, P. J. DeMott, A. J. Prenni, *J. Atmos. Sci.* **63**, 1752 (2006).
41. A. Seifert, K. D. Beheng, *Meteorol. Atmos. Phys.* **92**, 67 (2006).
42. A. Teller, Z. Levin, *Atmos. Chem. Phys.* **6**, 67 (2006).
43. W. K. Tao *et al.*, *J. Geophys. Res.* **112**, D24S18 (2007).
44. D. B. Johnson, *J. Atmos. Sci.* **39**, 448 (1982).
45. U. Lohmann, *Atmos. Chem. Phys.* **8**, 2115 (2008).
46. E. R. Graber, Y. Rudich, *Atmos. Chem. Phys.* **6**, 729 (2006).
47. V. T. J. Phillips, A. Pokrovsky, A. Khain, *J. Atmos. Sci.* **64**, 338 (2007).
48. M. W. DeMaria, *J. Atmos. Sci.* **42**, 1944 (1985).
49. D. Rosenfeld, W. L. Woodley, *Nature* **405**, 440 (2000).
50. A. P. Khain, D. Rosenfeld, A. Pokrovsky, *Geophys. Res. Lett.* **28**, 3887 (2001).
51. Z. Cui, K. S. Carslaw, Y. Yin, S. Davies, *J. Geophys. Res.* **111**, D05201 (2006).
52. A. P. Khain, N. BenMoshe, A. Pokrovsky, *J. Atmos. Sci.* **65**, 1721 (2008).
53. U. Dusek *et al.*, *Science* **312**, 1375 (2006).
54. E. Freud, D. Rosenfeld, M. O. Andreae, A. A. Costa, P. Artaxo, *Atmos. Chem. Phys.* **8**, 1661 (2008).
55. M. C. VanZanten, B. Stevens, G. Vali, D. H. Lenschow, *J. Atmos. Sci.* **62**, 88 (2005).
56. M. Wild *et al.*, *Science* **308**, 847 (2005).
57. D. G. Streets, Y. Wu, M. Chin, *Geophys. Res. Lett.* **33**, L15806 (2006).
58. The term "thermodynamic aerosol effect" was first mentioned in (*25*), but in a more restrictive context.
59. I. Koren, J. V. Martins, L. A. Remer, H. Afargan, *Science* **321**, 946 (2008).
60. B. Stevens, *iLEAPS Newsletter* **5**, 10 (2008).
61. The Aerosol Cloud Precipitation Climate (ACPC) initiative is a joint initiative by the International Geosphere/Biosphere Programme (IGBP) core projects Integrated Land Ecosystem/Atmosphere Process Study (iLEAPS) and International Global Atmospheric Chemistry (IGAC) and the World Climate Research Programme (WCRP) project Global Energy and Water Cycle Experiment (GEWEX).

62. This paper resulted from discussions held during an ACPC workshop hosted and supported by the International Space Science Institute, Bern, Switzerland, through its International Teams Program.

10.1126/science.1160606